

**NASA TECHNICAL  
MEMORANDUM**

**N 7 1 - 3 3 2 8 5**

**NASA TM X- 67902**

**NASA TM X- 67902**

**CASE FILE  
COPY**

**SHOCK TUBE TECHNIQUE FOR MEASURING OPACITIES AT HIGH  
PRESSURES FOR GASEOUS-CORE NUCLEAR ROCKETS**

by R. W. Patch  
Lewis Research Center  
Cleveland, Ohio

TECHNICAL PAPER proposed for presentation at  
Second Symposium on Uranium Plasmas sponsored  
by the American Institute of Aeronautics and Astronautics  
Atlanta, Georgia, November 15-17, 1971

# SHOCK TUBE TECHNIQUE FOR MEASURING OPACITIES AT HIGH PRESSURES FOR GASEOUS-CORE NUCLEAR ROCKETS

R. W. Patch  
Lewis Research Center  
National Aeronautics and Space Administration  
Cleveland, Ohio

## Abstract

A nonexplosive shock tube which should have higher performance than previous nonexplosive shock tubes is described. This shock tube should produce essentially homogeneous, isothermal gases or aerosols at conditions occurring in the propellant region in a gaseous-core nuclear rocket. The shock tube is currently under construction. A unique method of measuring the Planck and Rosseland mean opacities of shock tube gases without using high spectral resolution is derived. The selection of seed materials to be added to the gases to make them semiopaque is discussed.

## I. Introduction

In the gaseous-core rocket concept (fig. 1), hydrogen is heated by thermal radiation from a hot, fissioning uranium plasma located in the center of a chamber. Unfortunately, hydrogen is not sufficiently opaque at temperatures below 6000 K to prevent excessive thermal radiation from reaching the chamber walls and causing excessive wall heating. Hence the hydrogen is seeded with some material such as depleted uranium particles to increase its opacity. To assess the feasibility of the gaseous-core rocket, the opacities of uranium, hydrogen, and seed materials must be measured to compare with calculations. (1-7)

For temperatures of 8000 K and below, these opacity measurements should be made at high hydrogen densities approximating those in the rocket for four reasons: (1) At high temperatures some seeds form gaseous compounds with hydrogen. The concentrations of the compounds depend in a complicated way on the seed and hydrogen densities and the temperature. The compounds may have complex, overlapping spectra. (2) Some hydrogen optical absorption processes depend roughly on the square of the hydrogen density and hence are too weak to measure at low density. (3) Atomic hydrogen spectral lines are greatly broadened at high hydrogen densities due to neutral species. Broadening of a line effects the opacity. Theory and experiments on this broadening are few and unconvincing. (4) High hydrogen densities may broaden uranium,  $H_2$ , or seed vapor spectral lines substantially.

Successful measurements at elevated temperatures at these hydrogen densities have not been achieved in previous investigations. This paper describes an improved shock tube for accomplishing this which includes optics for a unique method for obtaining experimental Planck and Rosseland mean opacities without recourse to the difficult and laborious measurement of high-resolution spectral absorption coefficients.

## II. Shock Tube Design

Emphasis in the design was placed on obtaining a reproducible hydrogen partial pressure of 500 atm at reproducible temperatures from 2300 to 8000 K behind the reflected shock wave in a re-useable shock tube. A temperature of 8000 K at this hydrogen partial pressure is not attainable in any existing re-useable shock tube or ballistic piston compressor.

Based on Alpher and White's analysis<sup>(8)</sup> desired performance is achieved by the design shown in Fig. 2, which is essentially a high-purity state-of-the-art shock tunnel design without the tunnel and with a higher ratio of driver-to-driver cross-sectional area (4:1). The high performance is due to five techniques: (1) 4:1 ratio of areas as already mentioned, (2) high driver pressure, (3) use of hydrogen rather than helium as the driver gas because of its higher sonic velocity, (4) static heating of the driver gas to increase its sonic velocity still further, and (5) mixing of the optimum amount of the most appropriate inert gas with the hydrogen in the driven end to lower the gas's sonic velocity. The inert gas should have as high a molecular weight as possible without itself contributing significantly to opacity. This resulted in the selection of argon. The optimum amount was roughly two parts argon to one part hydrogen by volume.

Reproducibility of conditions behind the shock wave reflected from the right end (fig. 2) is obtained by careful mixing of gases, precise control of initial temperatures and pressures, and utilization of two scored metal diaphragms.<sup>(9)</sup> When two diaphragms are used, the buffer space between is filled with driver gas at half the driver pressure. To fire the shock tube, the firing valve is opened, so driver gas flows to the buffer, causing the righthand diaphragm to break. This causes a larger pressure difference across the lefthand diaphragm, so it breaks too. The resulting shock velocity is almost independent of the breaking point of the diaphragms within wide limits.

To determine the theoretical test time behind the reflected shock wave at the window (fig. 2), it is necessary to construct a wave diagram (fig. 3). Methods of constructing wave diagrams have been given by Rudinger.<sup>(10)</sup> Our wave diagram incorporates two refinements over Rudinger's methods: (1) conditions behind the incident and reflected shock waves were calculated with a computer program,<sup>(11)</sup> assuming chemical equilibrium and variable specific heat based on  $H_2$  energy levels given by Patch<sup>(12)</sup>; and (2) the steady and unsteady expansions in the vicinity of the convergence were treated by Alpher and White's more exact analysis.<sup>(8)</sup> The contact surface

in the wave diagram is the surface separating the test gas from the driver gas. The wave diagram in Fig. 3 is for 8000 K behind the reflected shock wave and shows that the expansion wave reflected from the end of the driver has no effect on test time. Instead, the theoretical test time is determined by the right-going expansion wave that results when the reflected shock wave passes through the contact surface and is 0.2 msec. (By careful selection of driver temperature or average molecular weights the right-going expansion wave could be eliminated, and the test time increased to about 1.2 msec.) The theoretical driver pressure is 995 atm.

A wave diagram constructed by similar methods for 2300 K behind the reflected shock wave looked quite different: the expansion wave reflected from the end of the driver determined the test time. This problem can be overcome by increasing the molecular weight in the driver.

Due to the high pressures of the test gas and the short test times needed for opacity measurements, boundary layer separation behind the reflected shock wave<sup>(13)</sup> is not expected to be a problem.

This shock tube is currently under construction.

### III. Method for Opacity Determinations

The two most important opacities in radiative transfer are the Planck and Rosseland means.<sup>(14)</sup> Approximate measurement of these opacities can be achieved for nongray gases without measuring high-resolution spectral absorption coefficients even if the gas has discrete spectral lines. Four requirements are that the gas be essentially isothermal, homogeneous, nonscattering, and in local thermodynamic equilibrium. The method involves a series of wide-band transmissivity measurements at different photon frequencies and different path lengths. Each wide spectral band is called a "group."

The derivation of an approximation for the Rosseland mean opacity  $a_{Ro}$  starts with the definition

$$\frac{1}{a_{Ro}} = \frac{\int_0^\infty \frac{1}{a_\nu} \frac{dB_\nu}{dT} d\nu}{\int_0^\infty \frac{dB_\nu}{dT} d\nu} \quad (1)$$

where  $a_{Ro}$  is in units of reciprocal length,  $a_\nu$  is the spectral linear absorption coefficient including stimulated emission,  $B_\nu$  is the Planck (or blackbody) function,  $T$  is the temperature, and  $\nu$  is photon frequency. Since  $B_\nu$  is a slowly varying function of frequency,

$$\frac{1}{a_{Ro}} \approx \frac{\sum_g \frac{1}{a_{Ro,g}} \frac{dB_g}{dT} \Delta\nu_g}{\sum_g \frac{dB_g}{dT} \Delta\nu_g} \quad (2)$$

where

$$\frac{1}{a_{Ro,g}} \equiv \frac{\int_g \frac{1}{a_\nu} d\nu}{\Delta\nu_g} \quad (3)$$

and

$$\bar{B}_g \equiv \frac{\int_g B_\nu d\nu}{\Delta\nu_g} \quad (4)$$

Here  $\Delta\nu_g$  is the frequency interval included in the group,  $g$  under an integral sign means to integrate over all frequencies in the group, and  $g$  under a summation means to sum over all groups.

Assuming a monochromator with a rectangular slit function and a fixed wavelength setting, or assuming a band-pass optical filter, the quantity measured in a photon absorption experiment is the group transmissivity.

$$T_g = \frac{I_g}{I_g^0} \quad (5)$$

where  $I_g^0$  is the incident intensity in frequency interval  $\Delta\nu_g$  and  $I_g$  is the intensity transmitted through a gas with path length  $S$ . Eq. (5) is equivalent to

$$T_g = \frac{\int_g I_\nu^0 e^{-Sa_\nu} d\nu}{\int_g I_\nu^0 d\nu} \quad (6)$$

If it is assumed that the incident spectral intensity  $I_\nu^0$  is constant in the frequency group, then

$$T_g = \frac{\int_g e^{-Sa_\nu} d\nu}{\Delta\nu_g} \quad (7)$$

from which it follows that

$$\int_0^\infty T_g dS = \frac{1}{a_{Ro,g}} \quad (8)$$

The integral in Eq. (8) can be evaluated numerically if  $T_g$  is measured for a number of values of path length  $S$ . (Extrapolation to infinite path length can be accomplished with an exponential.) Typical results for  $T_g$  for a nongray gas are shown in Fig. 4 and compared with a gray gas. Thus  $a_{Ro}$  of a nongray gas can be approximated by Eqs. (2), (4), and (8).

The derivation of an approximation for the Planck mean opacity  $a_{Pl}$  also starts with the definition

$$a_{Pl} = \frac{\int_0^\infty a_\nu B_\nu d\nu}{\int_0^\infty B_\nu d\nu} \quad (9)$$

In a similar manner

$$a_{Pl} \approx \frac{\sum_g \bar{a}_{Pl,g} \bar{B}_g \Delta\nu_g}{\sum_g \bar{B}_g \Delta\nu_g} \quad (10)$$

where

$$\bar{a}_{Pl,g} \equiv \frac{\int_g a_\nu d\nu}{\Delta\nu_g} \quad (11)$$

By a series expansion it can be shown that

$$\bar{a}_{Pl,g} = - \left( \frac{dT_g}{dS} \right)_{S=0} \quad (12)$$

which can also be obtained numerically if  $T_g$  is measured for a number of values of path length  $S$ .

Measurement of  $T_g$  in a shock tube for six values of  $S$  can be accomplished with mirrors as shown in Fig. 5, assuming the shock tube shots are reproducible so six shots can be used. Here the shock tube has inside diameter  $D$ , and two of the mirrors are secured to the shock-tube end wall and project into the interior of the shock tube. The flash lamp<sup>(15)</sup> produces a flash of about 15  $\mu$ sec duration, which is readily distinguished from the relatively constant photon emission from the hot gas behind the reflected shock wave in the shock tube. In practice, the flash lamp is fired first with a vacuum in the shock tube, and the monochromator output recorded. The shock tube is then filled and fired, with the flash lamp fired a few microseconds after passage of the reflected shockwave. Comparison of the monochromator output with the previous monochromator output gives the group transmissivity, assuming the flash lamp produces reproducible flashes.

There are several practical problems presented by the arrangement in Fig. 5. No high-intensity flash lamp reproduces its flashes exactly, so the group intensity of a reference beam (not shown) that does not pass through the shock tube must also be measured each time the flash lamp is fired. The reference beam is obtained by splitting the beam from the flash lamp before it goes through the shock tube.

Another problem is mechanical vibration due to firing the shock tube. This can cause misalignment of the optics,<sup>(16)</sup> invalidating the absorption measurements. It is not difficult to vibration isolate the flash lamp, monochromator, and mirrors external to the shock tube, but the internal mirrors cannot be vibration isolated. This

difficulty can be circumvented by replacing each internal mirror with a black surface at twice the distance from the right wall, disconnecting the flash lamp, and measuring group emissivity  $\epsilon_g$  instead of group transmissivity  $T_g$ . The two are related by

$$T_g = 1 - \epsilon_g \quad (13)$$

The frequencies (or wavelengths) to be included in the frequency groups should be the ones that contribute most to the radiant heat transfer in a gaseous-core nuclear rocket at distances from the wall where the gas temperature is from 2300 to 8000 K. These wavelengths must be estimated for design purposes. They were predicted by three methods and are shown in Fig. 6. For each method the shaded region contains 90 percent of the radiant heat transfer: 5 percent occurs at shorter wavelengths, and 5 percent occurs at longer wavelengths.

The most obvious method of predicting important wavelengths is to assume the radiant heat transfer at a given wavelength is proportional to the Planck function for the local gas temperature. The results are given in Fig. 6. The method would be correct if the gas were isothermal, gray, and optically thin, and the walls were cold.

A more realistic method is to assume that the gas is gray and the diffusion approximation<sup>(14)</sup> is valid. The radiant heat transfer at a given wavelength is then proportional to the contribution to  $1/a_{Ro}$  at that wavelength (eq. (1)). The results are given in Fig. 6.

The best method is to take a typical open-cycle gaseous-core nuclear rocket and compute the spectral radiant heat transfer by means of transport theory. This was done on a high-speed digital computer for a rocket with 1000 atm chamber pressure, chamber inside radius 1.2192 m, wall surface temperature 2777.7 K, and ratio of fuel volume to cavity volume of 0.25. The propellant was injected through the chamber walls at a rate of 20 kg/sec and consisted of 90 percent by mass hydrogen and 10 percent uranium particles to serve as seeds. The uranium particles were assumed to have an absorption coefficient of 50 000 cm<sup>2</sup>/g at all temperatures and wavelengths. Scattering of thermal radiation was neglected. Absorption coefficients for uranium and hydrogen were taken from Parks<sup>(4)</sup> and Patch,<sup>(2)</sup> respectively. The results are given in Fig. 6. By a slight extrapolation, it can be seen that for gas temperatures between 2300 and 8000 K, 90 percent of the radiant heat transfer falls between 0.2 and 2.2  $\mu$ m. Thus the frequency groups in Eqs. (2) and (10) should include these wavelengths.

#### IV. Opacities To Be Measured

A large number of opacity measurements are scheduled. They fall into six categories: (1) argon (as a check for impurities); (2) argon and hydrogen; (3) argon, hydrogen, and uranium hexafluoride; (4) argon, hydrogen, and a volatile compound containing a seed element other than uranium; (5) argon, hydrogen, and seed aerosols; and (6) argon, hydrogen, and seed aerosols of different kinds mixed to be as nearly gray as possible.

after they evaporate or react with hydrogen. The procedures for quantitative measurements of the absorption coefficients of aerosols in shock tubes are well established, (17-22) and measurements can be obtained on the aerosols before or after they evaporate or react with the carrier gas. However, producing and handling aerosols is more complicated than gas mixtures alone, so will be deferred until last.

The selection of seed materials to be tested depends on a number of factors. In a gaseous-core nuclear rocket, the seeds are always mixed with the hydrogen propellant injected through the chamber and exhaust nozzle walls. The seeds could be solid, liquid, or gaseous, but at injection temperatures gases have too low absorption coefficients and are not sufficiently gray to be suitable. Practically all previous experimental and theoretical studies of seed opacities have been performed on materials that are solids at injection temperature. (1) Seed materials should have high opacity, low neutron absorption, and low cost. They may be divided into reactive and non-reactive seeds according to whether they react or do not react extensively with hydrogen. A good reactive seed forms many compounds with hydrogen that have strong absorption bands. A good nonreactive seed has a high boiling point, and its vapor has many spectral lines and continua.

There are four currently favored seeds. Favored reactive seeds are silicon and carbon or graphite. Favored nonreactive seeds are depleted uranium and tungsten 184.

Someone familiar with rockets might think that the seed molecular weight would be very important because the seed vapor or reaction products flow through the exhaust nozzle along with the hydrogen propellant. However, calculations for an open-cycle gaseous-core nuclear rocket show that if the seeds are compared on the basis of opacity per unit mass, then the seed molecular weight is of negligible importance. This is shown in Fig. 7.

#### V. Conclusions

1. By using an improved shock tube design and a new method of opacity determination, it is feasible to measure the Planck and Rosseland mean opacities of hydrogen or seeded hydrogen at hydrogen partial pressures of 500 atm and temperatures of 2300 to 8000 K.

2. For an open-cycle gaseous-core nuclear rocket, the wavelengths important in radiant heat transfer are 0.2 to 2.2  $\mu\text{m}$  for gas temperatures from 2300 to 8000 K.

3. For an open-cycle gaseous-core nuclear rocket, the molecular weight of the seed added to the hydrogen propellant is of negligible importance if the seeds are compared on the basis of opacity per unit mass.

#### VI. REFERENCES

1. Patch, R. W., "Status of Opacity Calculations for Application to Uranium-Fueled Gas-Core Reactors," Research on Uranium Plasmas and Their Technological Applications, SP-236, 1971, NASA, Washington, D.C.
2. Patch, R. W., "Interim Absorption Coefficients and Opacities for Hydrogen Plasma at High Pressure," TM X-1902, 1969, NASA, Cleveland, Ohio.
3. Patch, R. W., "Calculated Pressure-Induced Vibrational Absorption in  $\text{H}_2\text{-H}_2$  Collisions in Hydrogen Gas," TN D-6155, 1971, NASA, Cleveland, Ohio.
4. Parks, D. E., Lane, G., Stewart, J. C., and Peyton, S., "Optical Constants of Uranium Plasma," GA-8244, NASA CR-72348, Feb. 1968, Gulf General Atomic, San Diego, Calif..
5. Main, R. P., "Optical Constants of Carbon-Hydrogen Mixtures," NASA CR-72570, May 1969, Heliodyne Corp., Van Nuys, Calif.
6. Main, R. P., "Opacity of Silicon-Hydrogen Mixtures," NASA CR-72749, May 1970, KMS Technology Center, Van Nuys, Calif.
7. Krascella, N. L., "Theoretical Investigation of the Absorptive Properties of Small Particles and Heavy-Atom Gases," NASA CR-693, 1967, NASA, Washington,
8. Alpher, R. A. and White, D. R., "Flow in Shock Tubes with Area Change at the Diaphragm Section," Journal of Fluid Mechanics, Vol. 3, P. 5, Feb. 1958, pp. 457-470.
9. Wurster, W. H., "Measured Transition Probability for the First-Positive Band System of Nitrogen," Journal of Chemical Physics, Vol. 36, No. 8, Apr. 15, 1962, pp. 2111-2117.
10. Rudinger, G., Wave Diagrams for Nonsteady Flows in Ducts, D. Van Nostrand, New York, 1955, pp. 1-208
11. Gordon, S., and McBride, B. J., "Computer Program for Calculation of Complex Chemical Equilibrium Compositions, Rocket Performance, Incident and Reflected Shocks, and Chapman-Jouguet Detonations," SP-273, (to be published), NASA.
12. Patch, R. W., "Components of a Hydrogen Plasma Including Minor Species," TN D-4993, 1969, NASA, Cleveland, Ohio.

13. Byron, S. and Rott, N., "On the Interaction of the Reflected Shock Wave with the Laminar Boundary Layer on the Shock Tube Walls" Proceedings of the 1961 Heat Transfer and Fluid Mechanics Institute, Binder, R. C., Epstein, M., Mannes, R. C., and Yang, H. T. (eds.), Stanford University Press, Stanford, 1961, pp. 38-54.
14. Penner, S. S. and Patch, R. W., "Radiative Transfer Studies and Opacity Calculations for Heated Gases," High Temperatures in Aeronautics, Pergamon Press, London, 1963, pp. 211-238.
15. Lalos, G. T., and Hammond, G. L., "Gas Opacity Measurements with a Ballistic Piston Compressor," NOLTR 70-15, NASA CR-72589, Nov. 1969, U. S. Naval Ordnance Laboratory, White Oak, Md.
16. Patch, R. W., "Absolute Intensity Measurements for the  $2.7 \mu$  Band of Water Vapor in a Shock Tube," Journal of Quantitative Spectroscopy and Radiative Transfer, Vol. 5, No. 1, Jan.-Feb. 1965, pp. 137-164.
17. Hickman, Roy S., "Progress on SAPAG Facility, II," Research Note 12, Dec. 1963, Heliodyne Corp., Los Angeles, Calif.
18. Louis, J. F., "An Alkali Metal Vapor Shock Tube and Measurements of the Conductivity and Electron Concentration of Cesium in Argon," Proceedings of the 5th International Shock Tube Symposium, U. S. Naval Ordnance Laboratory, Silver Springs, 1966, pp. 485-500a.
19. Hooker, W. J., Morsell, A. L., and Watson, R., "Shock tube Studies on Two-Phase Systems," Research Report 19, 1967, Heliodyne Corp., Van Nuys, Calif.
20. Hooker, W. J., Watson, R., and Morsell, A. L., "Measurements with Powdered Solids in Shock Tubes," Physics of Fluids, Vol. 12, No. 5, Pt. II, May 1969, pp. I-169-I-172.
21. Watson, R., Morsell, A. L., and Hooker, W. J., "Techniques for Conducting Shock Tube Experiments with Mixtures of Ultrafine Solid Particles and Gases," Review of Scientific Instruments, Vol. 38, No. 8, Aug. 1967, pp. 1052-1057.
22. Modica, A., Stepakoff, G., and Rosenbaum, H., "A Shock Tube Study of Plasma Alleviation by Oxide Dust," The Entry Plasma Sheath and Its Effects on Space Vehicle Electromagnetic Systems, Vol. I, SP-252, 1971, NASA, Washington, D.C., pp. 531-558.
23. Hooker, W. J. and Main, R. P., "BeO Oscillator Strengths," Final Report for Contract DAAH01-69-C-0096, Dec. 1968, Heliodyne Corp., Van Nuys, Calif.

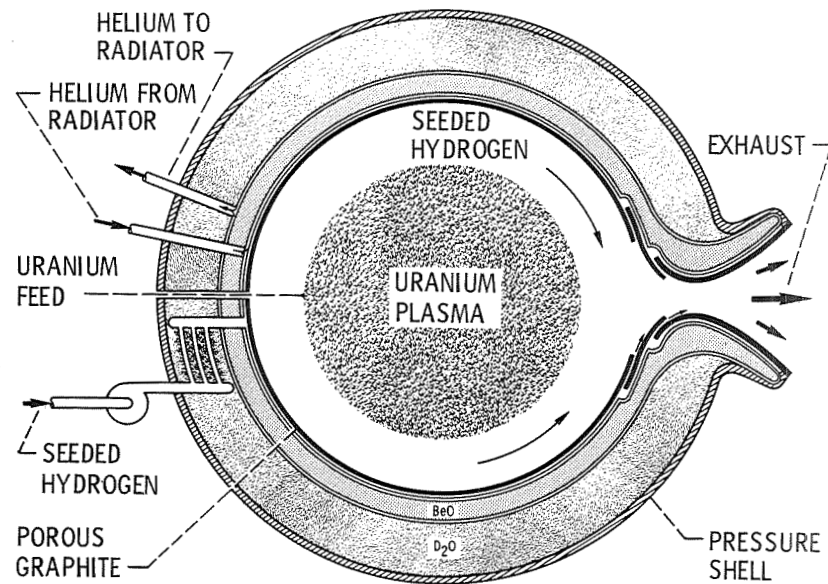


Figure 1. - Open-cycle gaseous-core nuclear rocket.

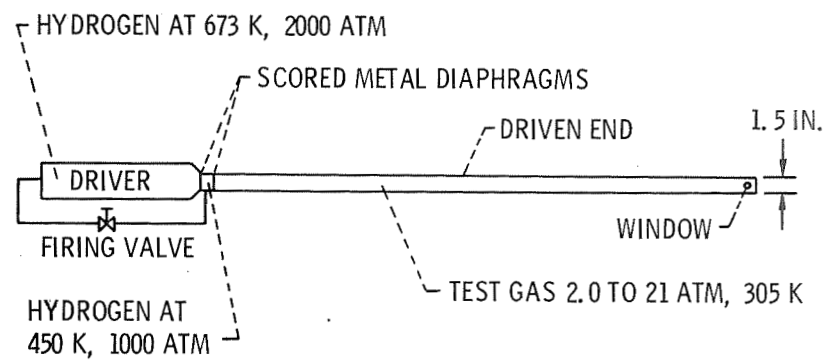


Figure 2. - Double-diaphragm shock tube for high-pressure transmission measurements (prior to firing).

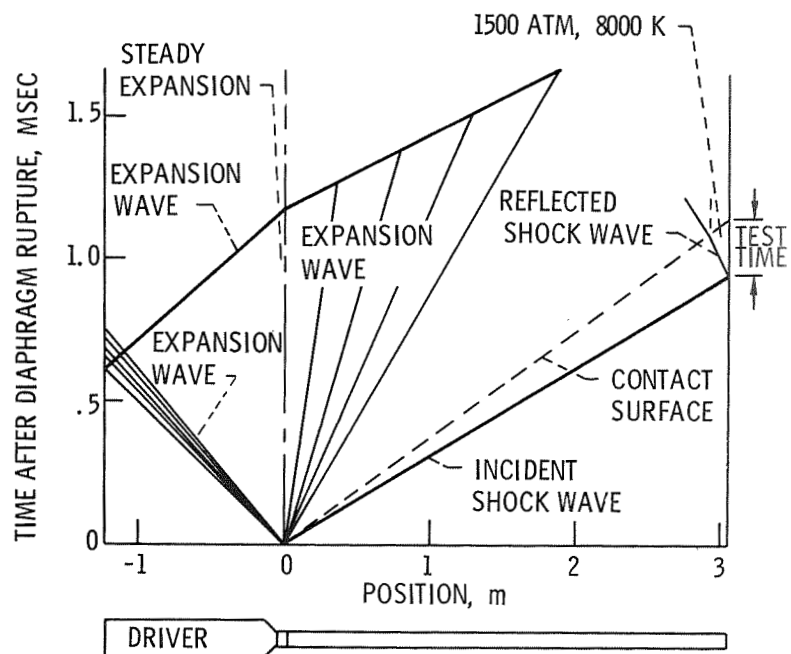


Figure 3. - Wave diagram for shock tube with convergence at diaphragm.

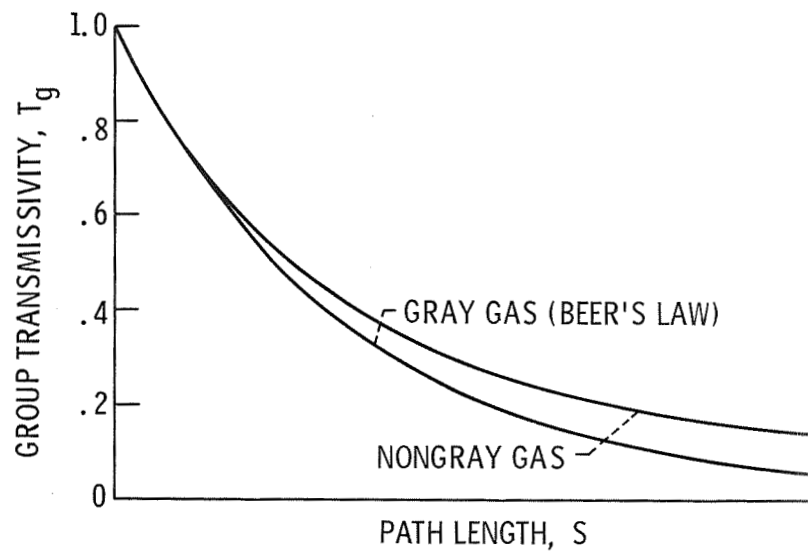


Figure 4. - Typical group transmissivities for gray and nongray gases.



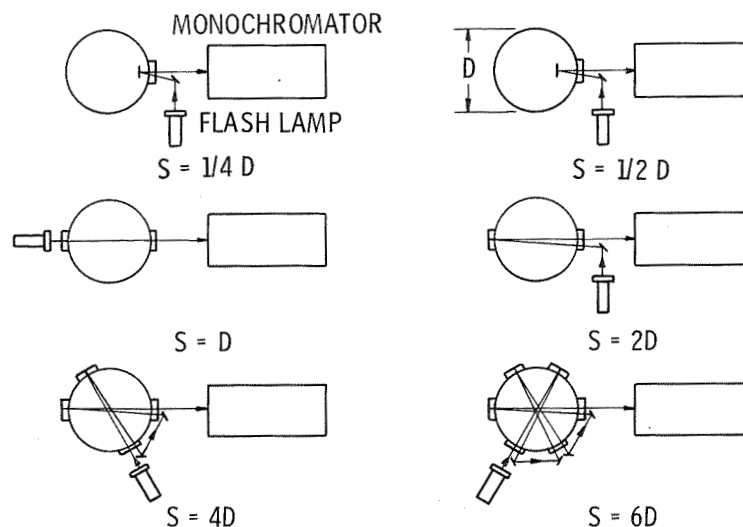


Figure 5. - Measurement of group transmissivities in gas near end wall of shock tube (schematic).

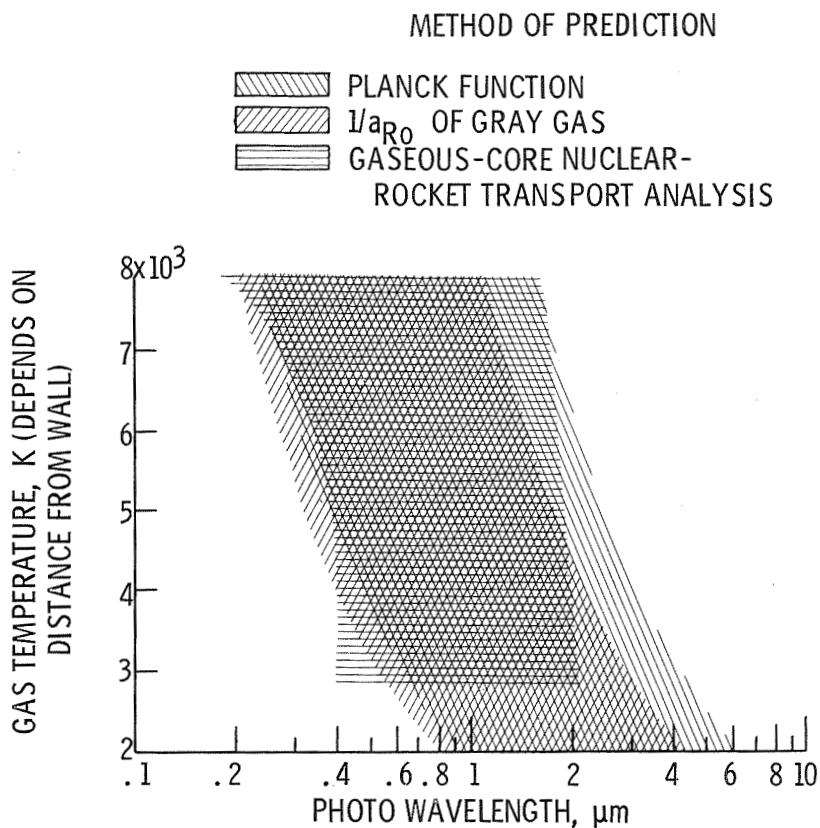


Figure 6. - Photon wavelengths that contribute 90 percent of radiant heat transfer in gaseous-core nuclear rocket predicted by three methods.

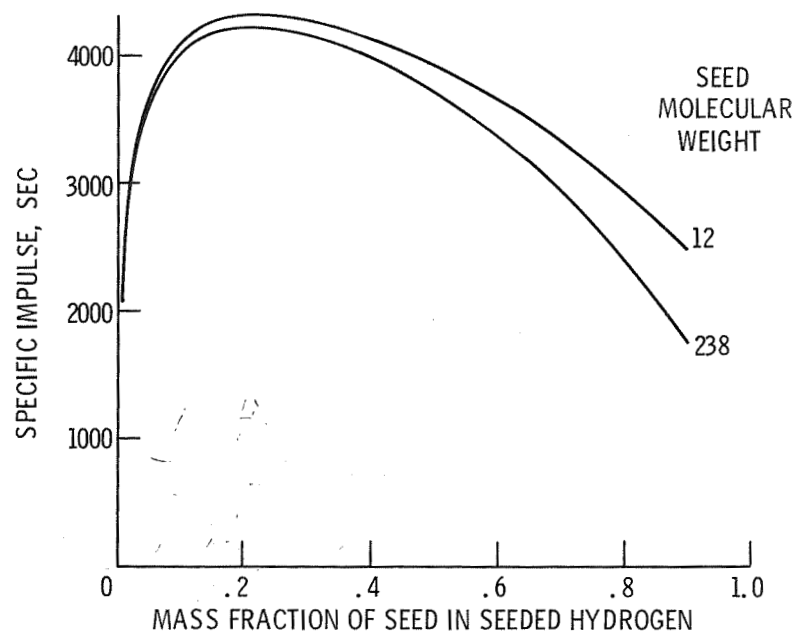


Figure 7. - Effect of seed molecular weight on specific impulse of gaseous-core nuclear rocket (seed particle opacity ( $\text{cm}^2/\text{G}$ ), seed vapor opacity ( $\text{cm}^2/\text{G}$ ), seed vapor pressure, and mass flow rates held constant).